Peer-reviewed version available at Sensors 2018, 18, 4042; doi:10.3390/s18114042

Review

EGFET based Sensors for Bioanalytical Applications: A Review

Salvatore Andrea Pullano[1,*], Costantino Davide Critello[1], Ifana Mahbub[2], Nishat Tarannum Tasneem[2], Samira Shamsir[3], Syed K. Islam[3], Marta Greco[1], Antonino S. Fiorillo[1]

[1] Department of Health Sciences, University "Magna Græcia" of Catanzaro, 88100, Catanzaro, Italy.
[2] Department of Electrical Engineering, University of North Texas, Denton, TX, USA.
[3] Department of Electrical Engineering and Computer Science, University of Missouri, Columbia, MO, USA.

* Correspondence: pullano@unicz.it; Tel.: +39–0961–369–4307

Abstract: Since 1970s, a great deal of attention has been paid to the development of semiconductor–based biosensors because of the numerous advantages they offer, including high sensitivity, faster response time, miniaturization, and low–cost manufacturing for quick biospecific analysis with reusable features. Commercial biosensors have become highly desirable in the fields of medicine, food, environmental monitoring as well as military applications (e.g. Hoffmann–La Roche, Abbott Point of Care, Orion High technologies, etc.), whereas increasing concerns on the food safety and health issues have resulted in the introduction of novel legislative standards for these sensors. Numerous devices have been developed for monitoring of biological–processes such as nucleic–acid hybridization, protein–protein interaction, antigen–antibody bonds and substrate–enzyme reactions, just to name a few. Since 1980s scientific interest moved to the development of semiconductor–based devices which also include integrated front–end electronics, such as the extended–gate–field–effect–transistor biosensor which is one of the first miniaturized chemical sensors. This work is intended to be a review of the state of the art focused on the development of biosensors based extended–gate–field–effect–transistor within the field of bioanalytical applications, which will highlight the most recent research works reported in the literature. Moreover, a comparison among the diverse EGFET devices will be presented giving particular attention to the materials and technologies.

Keywords: EGFET; ISFET; Electrochemical cell; Enzymatic biosensor; DNA–DNA biosensor; Immunosensor; Antigen–antibody biosensor; Ionic sensor.

1. Introduction

The earliest example of solid–for the sensing of ionic activities can be traced back to 1970 with the ion sensitive field effect transistor (ISFET), derived from an insulated gate field effect transistor (IGFET) [1]. In this class of devices, the gate consists of only a thin SiO_2 layer in contact with an electrolyte solution contained in an electrochemical cell, and the potential at the interface electrolyte/solution influences the drain current [1, 2]. The device as well as the electric connections is separated from the solution, avoiding possible damages caused by the penetration of liquids which guarantees the insulation from the external environment, as well as its biocompatibility. The information retrieved from the sample, in the first approximation the analyte concentration, depends on the interfacial potential with respect to an external reference electrode, which is part of the sensor itself. It provides a known, stable potential that does not depend on the intensity of the current (i.e. zero–current condition). The development of extended–gate–field–effect–transistor (EGFET) sprang from ISFET technology, and was first proposed by J. Van der Spiegel in 1983 [3].

Unlike ISFET, EGFET preserves the gate region as a standard metal–oxide–semiconductor–field–effect–transistor (MOSFET) and the sensing membrane is located

Peer-reviewed version available at Sensors 2018, 18, 4042; doi:10.3390/s18114042

on the outside [4]. Thus, the activity of target analyte results in an additional chemical contribution on the threshold voltage (V_{th}) [5]. The main applications of EGFETs are associated with the detection of ionic species, pH and specific molecules (through the functionalization of sensitive surfaces) such as urea and glucose [5–10]. Apart from its prevalent use in the field of biosensors, physical sensors for high frequency ultrasound detection (e.g. hydrophone) have been realized through the EGFET technology, often referred to as POSFET (piezoelectric oxide semiconductor field effect transistor) or PiGoFET (piezoelectric gate on a FET) [11–13].

The foremost problem with these solid–state devices is the threshold voltage drift which depends on the chemistry of the environment under test [14, 15]. This phenomenon manifests itself through a slow, continuous change in the threshold voltage of the device, usually in one direction. Different technical solutions have been proposed for its improvement by proposing different encapsulation techniques, even though until now there is no a general technology for the poor isolation between the device and the chemical environment. The most diffused involve multilayer materials such as the backside gate–type with Si–SiO_2–Si (SIS) [16], or silicon–on–sapphire (SOS) structure [17], [20]. Other techniques include the use polymeric membranes [18], photoresist [19], glass–bonded [21], and epoxy resin encapsulation [22]. Even though a great deal of the effort has been made with the aim of solving this limiting factor, the effects of drift remain a sticking point [14, 23]. Recently, introduction of microfluidics together with the integration of EGFET biosensors has made the packaging easier, with a reduction in the volume of the samples and reagents [24]. The following sections will look more closely at the principal components and relative functioning principles of EGFET, along with their foremost applications.

2. Fundamental Principles of EGFET

2.1. FET Device

The principal component of an EGFET device is a MOSFET, which confers long–term stability towards environmental variations (such as light and temperature), facilitates insulation and encapsulation, and makes it possible to vary the geometry of the sensing membrane more easily than the ISFETs [25–27]. The working principle is that of a conventional MOSFET, except for the sensing layer which is immersed in a buffer solution positioned at a certain distance from the device [28]. As can be seen in Figure 1(a), the device consists of a FET with high input impedance, a signal line (better if shielded), and the sensitive area connected to the gate [3]. EGFET allows the use of both on–chip integrated pre–amplifiers and, in the most recent configurations reported in the literature, discrete commercial–type devices connected to the gate extension. The latter is more precisely referred to as separative–extended–gate–field–effect–transistor (SEGFET) as shown in Figure 1(b). Sometimes, it is also named as ExGFET in order to avoid the ambiguity with electrolyte–gated field–effect transistor.

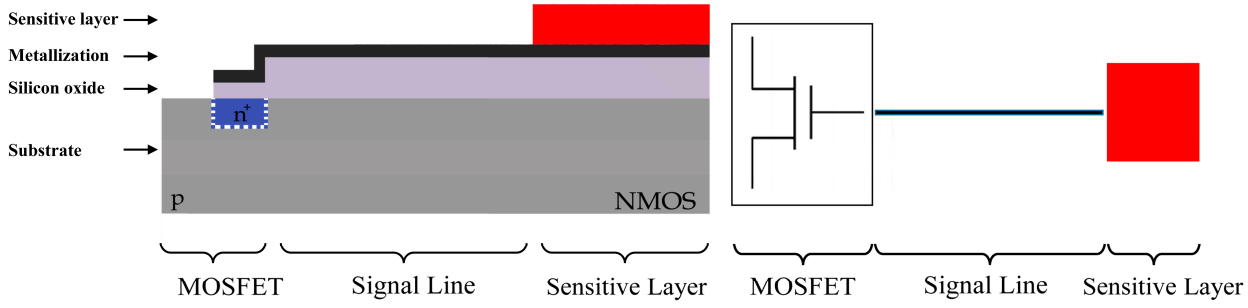

Figure 1. (**left**) Section of a device based on EGFET technology, (**right**) and a schematic of a SEGFET.

The impedance of the sensitive layer of EGFET is usually different from ISFET, in which it coincides with a high impedance gate dielectric. The sensitive layer (e.g. redox responsive material) of an EGFET is instead characterized by a low–impedance, with a consequently higher conductivity

and sensitivity. According to MOSFET literature, the equation that binds the channel current I_{DS} to the characteristics of the EFGET, usually in the linear region, is as follows:

$$I_{DS} = \mu C_{ox} \frac{W}{L}\left[\left(V_{\mathrm{Re}f} - V_{th}^{*}\right)V_{DS} - \frac{1}{2}V_{DS}^{2}\right] \quad (1)$$

where W and L are the width and length of the channel, μ is the mobility, C_{ox} is the gate oxide capacitance per unit area, V_{Ref} and V_{DS} are the applied reference electrode and the drain–to–source voltages, respectively. In Eq. (1), the only parameter linked to the analyte (i.e. activity of the analyte) is the overall threshold voltage V^{*}_{th} of the device [27, 28].

The aspect ratio W/L, and thus the transconductance, g_m, influences the performance of the device, particularly the input–referred–noise. High g_m values and consequently devices with a large surface area reduce the flicker ($1/f$) noise, which is implicated in surface conduction phenomena of the MOS caused by carrier recombination and interface traps. In fact, the oxide–semiconductor interface is characterized by random trapping and de–trapping of the carriers, that flow through the channel, generating flicker in the drain current. Since one of the aims of the EGFET is to further reduce the response time imposing the minimum possible channel length, the gate width can be modified increasing the aspect ratio. An empirical model for the evaluation of the power spectral density (PSD) of the flicker noise is expressed by the following model:

$$S_{I_{DS}} = \frac{M g_m^2}{C_{ox}^2 WL}\frac{1}{f^{\gamma}} \quad (2)$$

where f is the working frequency, M is an empirical parameter, and γ is a process parameter [29]. The PSD increases with the increase of the drain current depending on the region of operation, while large surface positively affects S_{IDS}. Humidity at high temperature has a different impact on the flicker noise depending on the channel type. Humidity affects flicker noise, mostly for p–channel devices while in n–channel, the contribution is negligible [30]. Therefore, the increase of W impacts on the performances, especially for low–frequency applications [12]. In addition to the flicker noise, both the device and the transduction interface are intrinsically affected by the thermal noise, depending on the leakage current at the oxide interface [12, 13]. Thermal noise spectral density have been investigated in MOSFET's by J. Van der Spiegel in strong, moderate and weak inversion regions in high W/L devices. The proposed model (valid only for "long channel" devices) highlighted that n–channel MOSFET is characterized by higher noise due to larger body effect apart of in strong inversion where the effect becomes less significant respect to p–channel device [31]. Latch–up and noise reduction can be obtained by properly bulk/well biasing and design layout. Apart from the noise ascribable to the FET, and eventually to the signal line if not properly shielded, EGFET sensor does not significantly suffer from other external interferences due to coupling from high–to–low impedance, since it is physically located near where the reaction takes place [32].

The possibility of designing ultra–short–channel EGFETs makes it necessary to revise and modify many of the corresponding long–channel counterparts in terms of channel doping, oxide thickness, potential distribution. Different empirical models have been proposed for adjusting the device parameters preserving the overall MOSFET behavior [33]. The length at which the long–channel behavior is maintained is as follow:

$$L \geq C\sqrt[3]{x_j t_{ox}\left(W_s + W_d\right)^2} \quad (3)$$

where C is a constant evaluated by fitting Eq. (3), x_j is the junction depth, and W_s and W_d are the source and the drain depletion depths (that can be subsequently designed), respectively [33]. The integration of a source–follower as an input stage together with a bootstrap reduces the input capacitance, which increases the overall sensitivity of the sensor [3]. Concerning the signal line, in the original design, it can be up to several millimeters long, thus the use of an insulating layer allows both electric and chemical shielding, reducing even cross–talk in the case of sensors located near each other [3]. This is even more actual in the most recent EGFET devices in which signal line

is even longer. Moreover, bootstrapping the shield means that there will be a less capacitive coupling between the signal line and the insulating shield also impacting the bandwidth of the sensor [34]. The threshold voltage V^*_{th} depends also on the typical parameters of the chemical environment in agreement with the following

$$V_{th}^{*} = V_{th} + E_{ref} + \chi_{sol} - \frac{W_M}{q} - \phi \quad (4),$$

where E_{ref} is the reference electrode potential, χ_{sol} is the superficial dipole potential of the electrolyte, W_M is the work function of the reference electrode, ϕ is the potential of the surface at the electrolyte/sensing membrane interface and q is the charge [2]. In other devices such as those exploiting the electrolyte–insulator–semiconductor (EIS) capacitive effect, an external electronic circuit is necessary to amplify the signal. Moreover, the equivalent capacitive model of the EIS is complex, notwithstanding its simple structure [35].

EGFET was designed as devices that had to improve the limits, in terms of output variability of ISFET, and their performance has been investigated under various conditions such as temperature [36], light exposure [28], and different chemical environment [25]. As compared to ISFETs, they have shown greater chemical and thermal stability as well as a better output stability under different incident light conditions, and increased current sensitivity [36, 37]. EGFET devices have been widely used in bioanalytical applications for detection of pH, enzymes and proteins [25]. As far as its design is concerned, different topology has been reported. In Figure 2, an example of an integrated circuit is shown in which the noteworthy dimensions of the gate electrode (sensitive area) are evident as compared to the source and drain electrodes.

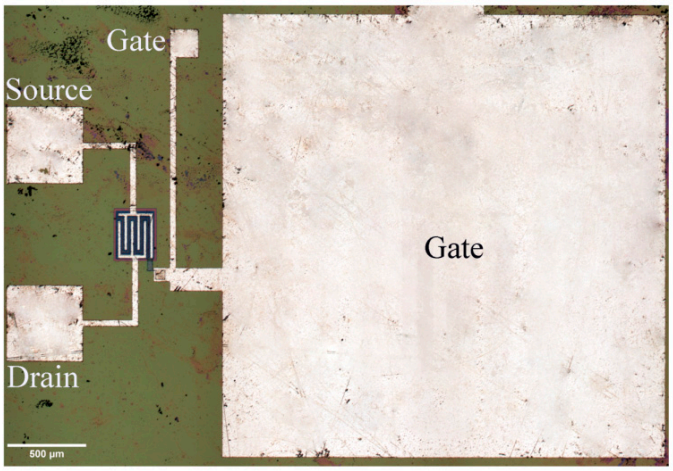

Figure 2. One of the first examples of an EGFET–based sensor realized in the 1980s. It is characterized by an aspect ratio of 1900/5 µm, originally fabricated for an integrated ultrasonic transducer, resulting from collaboration with Center for Sensor Technologies, University of Pennsylvania (courtesy of Prof. J. Van der Spiegel) [13].

2.2. Sensitive Layer

In bioanalytical applications, the potential of specific chemical species involved in the electrochemical reaction is transduced to an electric signal proportional to the target information (e.g. concentration) [38–42]. Depending on the electrochemical cell configuration chosen, the electric characterization can be performed through potentiometric, amperometric and conductometric schemes. The suitability of a particular configuration depends on the specific analyte, sensitivity and selectivity required, and the design of the overall system. The monitoring of the EGFET–based electrochemical cell requires one or more additional electrodes (i.e. reference and counter electrodes) besides the electrode where the reaction takes place (i.e. working electrode). Two electrodes configuration, the most commonly employed, can set detection limits due to limiting factors (e.g.

Preprints (www.preprints.org) | NOT PEER-REVIEWED | Posted: 12 October 2018 doi:10.20944/preprints201810.0251.v1

Peer-reviewed version available at Sensors 2018, 18, 4042; doi:10.3390/s18114042

overvoltage with respect to the zero current half–cell potential) [42]. One alternative solution is the use of three electrodes configuration by adding a counter electrode (e.g. amperometric scheme).

Potentiometric configuration is primarily involved in the evaluation of the potential across an interface, often a membrane [43, 44]. In direct potentiometry, the electromotive force is ideally a function of the activity of a single ion so that it can be selectively evaluated, even in the presence of other species. Most of the EGFET proposed in literature exploit potentiometric configuration as shown in Figure 3(a). In general, the system consists of a working electrode that has a sensitive layer or surface in which the electrochemical reaction takes place. The charge density on the surface of the sensing film will change the surface potential of the sensing film itself, modifying the characteristic curve of the transistor as well. More recently, ion–sensitive devices exploiting floating–gate without the use of a reference electrode have been investigated by applying a bias voltage to a control gate rather than a reference electrode [45, 46].

Typical characteristic curves for an ion–sensitive EGFET is shown in Figure 3(b) in which the current–voltage characteristics of the transistor change depending on the analyte, and the input signal is assessed by the transfer characteristics (I_D–V_{Ref}) using a semiconductor parametric device analyzer.

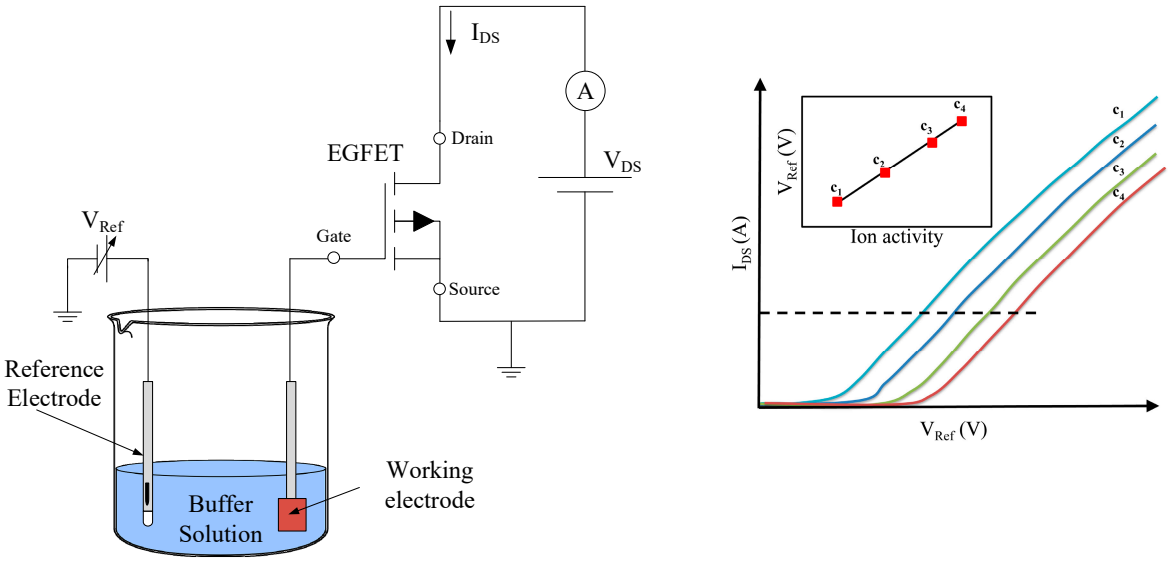

Figure 3. (**a**) Typical setup for EGFET based potentiometric sensor system. (**b**) Transfer characteristics (I_{DS}–V_{REF}) of an analyte sensitive EGFET at different concentration. In the insect is reported the dependence of concentration with respect to the reference voltage.

The most frequently employed electrodes (especially those used as reference) are fabricated in Ag/AgCl because of their smaller size, simpler fabrication and integration into the device. In addition, these electrodes are not susceptible to the corrosion phenomena of the solution. Other electrodes are hydrogen, saturated–calomel (SCE) based on elemental mercury and mercury (I) chloride, copper/copper sulfate or palladium/hydrogen electrodes. However, the reference electrode does not have a stable potential depending on the circulating current, but the use of high input MOS interface minimizes any leakage current that can change its potential.

Working electrode materials play an important role concerning the specific biosensors to be fabricated. Materials can be categorized as metal based, carbon based, and polymer based electrodes. In many cases reported in literature, the working electrodes are functionalized with nanomaterials and mediators to enhance sensitivity and selectivity. Working electrodes based on metal oxides (insoluble and stable in solution), as discussed with more details later, have been classically investigated for pH sensors and represent one of the widespread applications involving EGFET devices [4, 6, 7]. The general approach largely accepted is based on the theory of the electric double layer and the electric charge gathered at the oxide surface. It is valid for metal oxides whose charging mechanisms follow the association–dissociation of an amphoteric group [2]. Apart from pH detection, the investigation of sensitive layers functionalized with biological molecules (e.g.

Peer-reviewed version available at Sensors 2018, 18, 4042; doi:10.3390/s18114042

enzymes, antibodies, nucleic acids) allows specific binding or catalytic reactions resulting in electron transfer related to the specific analyte or a group of analytes (e.g. usually oxidases). Functionalized bio–selective surface overcomes the slow kinetics of the target molecules even though more recently enzyme–free electrodes have also been investigated with good results. There are a variety of available enzymes and each one is appropriate to catalyze an electrodic reaction in the presence of a specific analyte. In Table 1 a few representative substrates investigated for the fabrication of sensitive surfaces, the related enzymes, the target molecules and the immobilization techniques adopted are reported. The ability to catalyze a large number of reactions not being consumed, allowing a "continuous" use of the device is one of the main reasons for the common use of enzymatic biosensors. However, the lifetime of the sensor is limited by the stability of the enzyme.

Table 1. Electronic Materials Used for Working Electrodes.

Ref.	Substrate	Functionalization	Target	Method of immobilization
[47]	Au/Ag–NWs	HRP	Hydrogen peroxidase	Covalent bonding
[57]	Carbon/ZnO	Hb		Covalent bonding
[63]	GC/Ag NPs/MWNTs	Hb		Entrapped
[64]	Graphene/Au–NPs	Enzyme–free		
[66]	Nafion modified GC/CNT	Enzyme–free		
[48]	Au/Ag–NCs	HRP/GOx	Glucose	Entrapment
[52]	ITO/CS–PPy Au–NPs	GOx		Entrapment
[53]	Ag/CNT/CS	GOx/HRP		Layer technique
[55]	BDD/Graphene/Pt–NPs	GOx		Adsorption
[58–62]	Si/VACNFs	GOx/HRP		Adsorption
[65]	Graphite NPs	GOx		Covalent bonding
[49]	Pt/Pt–NPs–PPy	SOx	Sulfite	Entrapment
[50]	ITO/PEDOT:PSS	TPM	Dopamine, Ascorbic acid	CVD
[51]	FTO/GONPs–PPy	BOx	Bilirubin	Entrapment
[54]	GC	DHB	Adenine Dinucleotide	Potential activation
[56]	BDD/MWCNTs	Tyrosinase	Bisphenol A	Entrapment
[67]	GC/PEDOT/MWCNTs	SOD	Wine antioxidants	nr

NW: Nano–Wall, GC: Glassy Carbon, NP: Nano–Particle, MWNT: Multi–Walled Carbon Nano–Tube, CNT: Carbon Nano–Tube, NC: Nano–Cube, CS: Chitosan, PPy: Polypyrrole, BDD: Boron Doped Diamond, VACNF: Vertically Aligned Carbon Nano–Fiber, PEDOT:PSS: poly(3,4–ethylenedioxythiophene) polystyrene sulfonate, GONP: graphene oxide nanoparticle, HRP: Horse Radish Peroxidase, CS: Chitosan, Hb: Hemoglobin, , GOx: Glucose Oxidase, Box: Bilirubin Oxidase, Sox: Sulfite oxidase, TPM: 3–(trichlorosilyl) propyl methacrylate, CVD: Chemical vapor deposition, DHB: 3,4–dihydroxybenzaldehyd, SOD: superoxide dismutase. nr: not reported

Recent literature also reported a further classification of enzymatic sensors into three successive generations of devices: the first limited by nonspecific electroactive particles, the second, in which mediators are employed as electron carriers, and the third, in which there is a direct electron transfer between the electrode and the enzyme (absence of mediators) [68]. In addition to biosensor –devices which exploit –catalytic enzyme activity, molecular interactions such as antigen–antibody reactions (immunosensor) and nucleic acid interactions (genosensors, also referred to bio–affinity devices), represent a field of increasing interest for EGFET based devices. Single–stranded DNA/RNA segments of 20–40 base pair, highly target–selective, are immobilized on the electrode surface retaining their stability, reactivity, accessibility to the target analyte and optimal orientation. When target DNA binds to the complementary sequence (the so–called hybridization), a DNA–mediated electron transfer takes place through the DNA nucleotides/bases on electrode surface usually involving current monitoring at a fixed potential.

3. Applications of EGFET–Based Biosensors

3.1. pH Sensors

pH is an extremely important biological parameter for the human health, providing information for the diagnosis of many diseases as well as for the enhancement of therapeutic treatment. It can also be used as a tool for the monitoring of biological and biochemical processes. One of the foremost recent examples concern tumor cells, for which an elevated pH is an indicator of the onset of tumor cell proliferation [69, 70]. Monitoring of pH levels of living cells is also important in case of endocytosis and phagocytosis [71, 72]. Among the analytical models developed so far, the most widespread is the *site–binding* model, which was first introduced by Yates in 1973 (i.e. *site–dissociation* model) and then further developed by the same group. The model describes the electric double layer at the oxide–electrolyte interface, supposing an amphoteric oxide layer [73]. The pH of the electrolyte solution influences the hydroxyl groups at the surface (i.e. sensing membrane potential) as follows:

$$-2.303\Delta pH = \frac{q\phi}{kT} + \sinh^{-1}\left(\frac{q\phi}{kT\beta}\right) \quad (5),$$

where $\Delta pH = pH_{PZC} - pH$, pH_{PZC} corresponds to the pH value for which the surface charge is null, k is the Boltzmann's constant, T is the temperature and β is the buffer capacity, a parameter that characterizes the ability of the sensitive surface to buffer pH changes (β is an inherent property of the sensing material). According to the *site–binding* model, the number of binding sites on the sensing membrane can change the potential of the electrolytic interface, as well as the potential of the sensing membrane, that is expressed by [74]:

$$\phi = 2.303\frac{kT}{q}\frac{\beta}{\beta+1}\left(pH_{PZC} - pH\right) \quad (6)$$

The difference in potential between the reference electrode and the sensing membrane is $V_{out}=V_{ref}-\phi$ [75]. The applications of pH sensors are numerous. For example, they are used in the monitoring of the quality of drinking water, soil analysis or in the inspection of processes in the food industry [76, 77]. Different oxide substrates have been used as sensing membranes, among which tantalum oxide (Ta_2O_5), indium–tin oxide (ITO), tin oxide (SnO_2), platinum dioxide (PtO_2), vanadium anhydride (V_2O_5), xerogel, niobium oxide (Nb_2O_5), zinc oxide (ZnO), titanium dioxide (TiO_2), and ruthenium oxide (RuO_2), just to name a few [36, 37, 78–90]. To further reduce the manufacturing costs, particularly those of the sensing membrane, recycled materials from other sectors have also been investigated. Industrial–grade touch panel film (TPF) is an example. TPF is a multi–layered material composed of ITO/SiO_2/Nb_2O_5 that has several advantages when used as a pH sensor such as good sensitivity and high response speed [91]. As already mentioned, the list of the materials used as a sensing membrane is very long, and the choice depends mainly on the range of interest and the required sensitivity [82, 91–96]. Most of the efforts reported in the literature have been addressed to improve the performance of the EGFET–based pH sensors with the use of different materials including composites. The buffer capacity β has been intensively investigated to improve the sensor sensitivity. According to the literature, it can be expressed as:

$$\beta = \frac{2q^2 N_s \sqrt{K_a / K_b}}{kTC_d} \quad (8)$$

where N_s is the surface site numbers, K_a and K_b are equilibrium constants and C_d is the differential capacitance of the electrolyte, which account for the storage of electric charge after experiencing electrostatic potential. The buffer capacity and the differential capacitance mostly affect the pH sensitivity of the sensor, leading to a maximum sensitivity for $\beta >> 1$, which is limited to 59 mV/pH @ 297 K (the so–called Nernst limit) [97–99]. Nevertheless, literature reports materials which show

283 super–Nernstian sensitivity [100]. Table 2 shows a few representative pH sensors based on EGFET
284 with particular emphasis on the materials technology, the FET device and the overall biosensor
285 characteristics.

286 **Table 2.** Main Characteristics of Some Types of pH Sensors.

Ref.	Sensitive material	Sensitivity (mV/pH)	Range	Linearity (%)	Drift (mV/h)	Hysteresis (mV)	Reference electrode	Sensitive area	FET device	Type
[27]	ITO	58	2–12	nr	nr	9.8	SCE	6 mm^2	CD4007UB	P
[28]	SnO_2	56–58	2–12	nr	nr	nr	SCE	nr	CD4007UB or LF356N	P
[36]	TiO_2	59.89	2–12	93.50	0.041692 –2.6007	5.3–9	Ag/AgCl	1 cm^2	NDP6060L	P
[37]	V_2O_5	58.1±0.8	2–12	nr	nr	nr	nr	nr	CD4007UB	P
[79]	ITO/PET	50.1±1.7	2–12	98.5	13.2	nr	Ag/AgCl	$\Pi \times 2^2$ mm^2	CD4007CN	P
[81]	ITO/PET	45.9–52.3	2.1–12.1	98.3–99.6	nr	nr	Ag/AgCl	$\Pi \times 2.5^2$ mm^2	CD4007UB	P
[82]	SnO_2	59.3	2–9.4	nr	nr	nr	Ag/AgCl	nr	LT1167 – I.A.	P
[88]	AZO	57.95	1–13	99.98	4.83	1.27	Ag/AgCl	2×2 mm^2	CD4007UB	A
[91]	ITO/SiO_2/Nb_2O_5	59.2	3–13	99.48	2 %	1.83 %	Ag/AgCl	20×20 mm^2	IC4007	P
[93]	ZnO Nanorods	45	4–12	nr	nr	nr	Ag/AgCl	$\Pi \times 2.5^2$ mm^2	CD4007UB	P
[95]	SnO_2/SiO_2/glass	58	1–9	nr	nr	nr	Ag/AgCl	1.5×1.5 mm^2	LT1167 – I.A.	P
[96]	SnO_2/ITO/PET	53.8–58.7	2–12	nr	nr	nr	Ag/AgCl	nr	LT1167 – I.A.	P
[100]	PdO	62.87±2	2–12	99.97	2.32	7.9mV	Ag/AgCl	0.25 cm^2	CD4007UBE	P
[101]	InGaZnO	59.5	2–10	99.7	3–9	nr	Ag/AgCl	nr	CD4007	P
[102]	Glass	55	2–12	nr	nr	nr	nr	nr	CD4007UB	P
[103]	CNT	50.9	3–13	99.78	nr	nr	nr	1×2 cm^2	nr	P
[104]	FTO	54.10	2–12	nr	nr	nr	nr	nr	CD4007UB	P

287 P: Potentiometric. A: Amperometric. I.A: Instrumentation Amplifier. nr: not reported

288

As shown, there are a wide number of usable sensitive layers which can provide the development of even more tailored sensor solutions for the specific application. Furthermore, EGFET–based sensors can be importantly miniaturized and can be suitably integrated into different microsystems.

3.2. Urea Sensors

Urea is generally known as the best indicator for the evaluation of the level of uremic toxins in the bloodstream. Different types of biosensors have been proposed for urea detection; especially based on ISFET and ENFET (ENzymatic Field Effect Transistor) [6, 105, 106]. Urea sensors are widely used in the medical diagnostics for pathologies such as kidney failure, leukemia, diabetes and hyperthyroidism [107]. Urease is the specific immobilized enzyme used for the detection of urea, following the reaction:

$$CO(NH_2)_2 + 3H_2O \xrightarrow{urease} 2NH_4^+ + HCO_3^- + OH^- \quad (9)$$

Urease catalyzes the hydrolysis of urea, which can be determined through a change in pH or in the concentration of ammonium ions. Urease is immobilized on the sensing membrane by different methods such as physical adsorption, entrapment, covalent bonding and cross–linking [108–112]. Lately, in order to simplify the production process and to improve the efficiency of the enzyme/analyte bonds, urea sensors based on EGFET have been developed [82, 113]. Covalent bonding is a very effective method of immobilization due to the strong interaction that comes between the enzymes and the biological material, giving to the biosensors longer time stability. Nevertheless, alternative low–cost (inorganic) methods have been developed, including plasma–treatment (e.g. plasma enhanced chemical vapor deposition) of ITO/polyethylene terephthalate (PET) substrate which creates amino bonds on the surface and immobilizes urease [81, 114]. Chen et al. have developed urea sensor based on EGFET technology using a structure made of tin dioxide (SnO_2), ITO and glass as sensing electrodes characterized by a response time of 1–2 minutes with high immunity to variations of light and temperature [82]. Besides tin oxide, tin oxide doped with fluorine atoms (FTO) has also been used as a sensitive material on EGFET sensors, obtaining a pH sensitivity of 54.10 mV/pH (pH range from 2 up to 12) and urea sensitivity of 8.92 μA/pC_{urea} (see also Table 3) [104].

Table 3. Main characteristics of some representative urea sensors.

Ref.	Sensitive material	Sensitivity	Range (mM)	Linearity (%)	Reference electrode	Sensitive area	FET device	Type
[81]	ITO/PET	21.2 mV/pCurea 49.7 mV/pCurea 62.4 mV/pCurea	0.5–10	96.5 99.0 98.6	Ag/AgCl	Π × 2.5² mm²	CD4007UB	P
[82]	SnO_2/ITO	nr	0.05–20		Ag/AgCl	nr	LT1167 – I.A.	P
[96]	SnO_2/ITO/PET	≈40 mV/mM	0.04–0.33	97	Ag/AgCl	nr	LT1167 – I.A.	
[104]	FTO	8.92 μA/pCurea	0.01–300			nr	CD4007UB	A

P: Potentiometric. A: Amperometric. I.A: Instrumentation Amplifier. nr: not reported.

Being of clinical interest (especially in the blood), EGFET–based urea sensors can represent a promising technology (especially for the development of disposable devices) that indirectly detects urea concentration through the evaluation of pH variation as a result of an enzymatically catalyzed reaction.

3.3. Glucose Sensors

The first biosensor for the measurement of glucose was described by Clark and Lyons in 1962 [115]. The principle of detection is based the generation of gluconate and hydrogen peroxide (H_2O_2) catalyzed by glucose oxidase enzyme (GOD) in a glucose solution. By means of a dissociation reaction of H_2O_2, the potential of the sensing membrane change. The chemical reaction, catalyzed by the GOD enzyme, is as follow:

$$Glucose + O_2 \xrightarrow{GOD} Gluconic\_Acid + H_2O_2 \quad (10)$$

$$H_2O_2 \rightarrow O_2 + 2H^+ + 2e^-$$

Zinc oxide (ZnO) is one of the common materials used for the fabrication of the sensing membrane. In order to increase the conductivity of this membrane, the zinc oxide can be "*loaded*" with metallic elements. When aluminum is chosen, it is referred to as AZO (Aluminum–doped ZnO). Table 4 reports some representative characteristics of the EGFET based on AZO or ZnO nanostructures for glucose detection as a function of the process temperature.

Table 4. Effect of temperature on glucose sensors based on AZO and ZnO nanostructures.

Ref.	Sensitive material	Sensitivity (μA mM^{-1} cm^{-2})	Range (mM)	Linearity (%)
	Low Temperature			
[88]	AZO nanowires	60.5	0–13.9	99.96
[116]	ZnO nanowire	23.43	00.1–5.9	99.52
[117]	ZnO nanotube	30.85		99.99
[88]	ZnO nanotube	21.7	0.05–12	99.8
	High Temperature			
[118]	ZnO micro/nano wires	89.74	0.1–0.59	99.76
[119]	ZnO nanonails	24.613	0.1–7.1	99.37

Due to its clinical interest and an electrically favorable chemical reaction, glucose sensors have been widely investigated on different biological fluids (e.g. blood, saliva, tears, sweat). Table 5 presents the main characteristics of EGFET–based glucose sensors with particular emphasis on materials and performances.

337 **Table 5.** Main characteristics of some representative EGFET–based glucose sensors

Ref.	Electrode	Sensitivity	Range (mM)	Linearity (%)	Drift (mV/h)	Hysteresis (mV)	Reference electrode	Sensitive area (μm²)	FET device	Type
[88]	AZO	60.5 μA mM−1 cm−2	up to 13.9	99.96	1.27	4.83	Ag/AgCl	$2 \times 2 \cdot 10^6$	CD4007UB	A
[106]	Au	–61.6 mV/decade	0.125–1	99.60	nr	nr	Ag/AgCl	10 × 10	0.6 μm CMOS	P
[120]	PPI/NiTsPc	128 mV/mM	0.05–1	Nr	nr	nr	Ag/AgCl	Nr	AD620 I.A.	P
[121]	Au	58 mV/decade	0.1– 2	99.99	0.50	nr	Ag/AgCl	20 × 56	32 x 32 array 1.2 μm CMOS	P
[122]	Ru doped TiO2	320 μV/(mg/dL)	5.55–27.55	99.50	nr	nr	Ag/AgCl	$2 \times 2 \cdot 10^6$	LT1167 I.A.	P
[123]	ZnO	20.33 μA mM−1 cm−2	0.5–10	nr	nr	nr	Ag/AgCl	nr	CD4007UB	P
[124]	ZnO Nanorods	nr	0.01–5	nr	nr	nr	Ag/AgCl	nr	Glass FET	P

338

339 P: Potentiometric. A: Amperometric. I.A: Instrumentation Amplifier. nr: not reported. PPI/NiTsPc: poly(propylene imine) dendrimer/nickel tetrasulphonated phthalocyanine

3.4. Calcium Ion Sensors

Calcium ions regulates a series of biological processes such as cell proliferation, gene expression and apoptosis through bonding interactions with specific proteins, each one having a different affinity [125]. The proteins that bind with calcium are found both inside and outside of the living cells, although it acts as a "trigger" for the abovementioned processes [126]. Sensing nanostructures based on semiconductors offer advantages in terms of biocompatibility, time response, and miniaturization (see Table 6). Various materials have been used to realize sensing membranes for these sensors. For instance, zinc oxide was used for the realization of "*nanorod sensors*", developed to measure the concentration of intra– and extra–cellular calcium ions [86, 132]. These sensors, integrated on FETs with a separate extended gate, have shown themselves to be linear and sturdy.

Table 6. Sensors of Calcium Ions

Ref.	Sensitive material	Sensitivity	Range	Linearity (%)	Reference electrode	Sensitive area (mm^2)	FET device
[129]	RuO_2	32.5 mV/pCa	pCa0–pCa2	97.6	Ag/AgCl	nr	NMOS
[130]	Ru–doped TiO_2 or RuO_2	29.65 mV/pCa	pCa0–pCa3	99.9	Ag/AgCl	nr	CD4007UB
[131]	SnO_2	0.156 mV/pCa	1.16–1.31 mM	>99.85	Ag/AgCl	nr	CD4007UB
[132]	ZnO nanorods	26.55 mV/decade	0.001–100 mM	nr	Ag/AgCl	$\Pi \times 0.25^2$	nr

nr: not reported.

3.5. DNA Sensors

Nucleic acid biosensors find wide application for the identification of pathogens, pharmaceutical screening and diagnosis of genetic diseases, as well as the virus and tumor cell detection. The working principle of these sensors is based on the specific recognition of a single short chain of nucleic acids that hybridizes with complementary DNA/RNA strand. FET technology for acid nucleic detection is mostly characterized by sensing membranes capable of amplifying the events of nucleic acid hybridization. For instance, an EGFET device with an Au nanoporous membrane has been recently proposed for the evaluation of *Staphylococcus aureus* 16S rRNA (see Figure 4). The presence of this membrane gives the device high linearity, a broad dynamic range (from 10 pM to 10^6 pM) a limit of detection of ~1 pM [133]. Sensing membranes based on nanowires and nanofilms have been investigated recently as a part of an extended–gate device. Gallium nitride (GaN) was used because of its biocompatibility and non–toxicity. Both biosensors exhibited high selectivity and rapid detection, even though those fabricated with nanowires were more sensitive showing a wide dynamic range (from 10^{-7} pM to10^6 pM) [134].

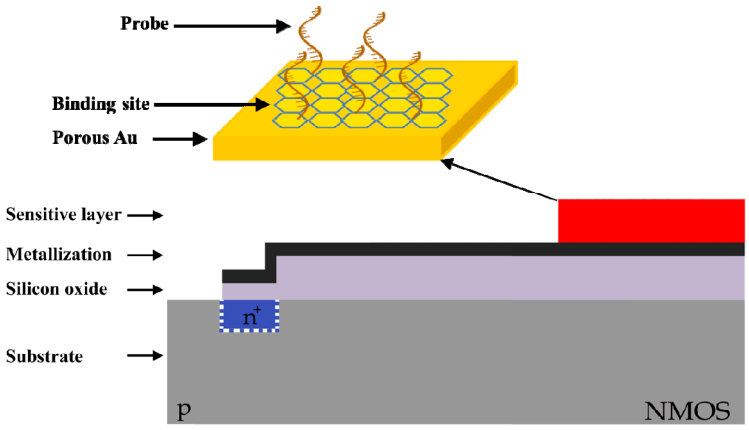

Figure 4. Schematic of an EGFET for DNA sensing using a nanoporous gold layer with binding site (e.g. thiole) for enhancing probe immobilization [133].

3.6. IImmunosensors

Immunosensors belong to a class of biosensors based on antigen–antibody interaction in biological fluids and is a well–recognized, and consolidated technology in the field of clinical diagnostics. These biosensors are also used in applications inherent to environmental pollution and food safety when the analyte is a microorganism such as bacteria, virus, or herbicide. Recently, an immunosensor has been developed and characterized using SEGFET technology for the detection of a dengue virus nonstructural protein 1 (NS1) [135]. This sensor consists of the previously discussed separate extended–gate terminal (gold electrode), modified with anti–NS1 antibodies. This device has shown a linear current response for concentrations of less than 1 μg/ml with a detection limit of 0.25 μg/ml. The fabricated device and the similar, which are reported in the most recent literature, suggests the possibility of using this biosensor as an alternative to the conventional techniques that require adequate instruments and trained personnel.

4. Discussion and Conclusions

The presented survey of the most recent advancements on EGFET based sensors represents an attempt, not exhaustive, of the current efforts in this field. The origin of biosensors can be traced back to approximately 60 years ago when Clark and Lyon realized electrodes that were able to recognize enzymatic structures [115]. Since then, the scientific community has been developing even more trustworthy biosensing devices that are increasingly responsive to biological species. As highlighted in the previous sections, the development of these devices is currently in expansion thanks to the implementation of even more sophisticated nano–technologies derived from electronics, physics and science–of–materials. This class of sensors, particularly the potentiometric devices using FET technology, are more easily miniaturized as compared to other types of biosensors (optical, thermal, etc.), justifying the strong scientific interest currently manifested in the field of biomedical research. In general, the use of FETs allows the low–cost transduction of biological information by means of a specific interaction between the sensitive element and the analyte, avoiding cumbersome and complex instruments, reducing chemical reagents and specific markers (label–free). Van der Spiegel highlighted the important key points concerning the development of a new class of monolithic sensors utilizing novel FET devices which include the fabrication of a sensitive layer with high specificity for the desired chemical species, which is placed separately from the transistor, avoiding possible damages caused by the surrounding chemical environment. This is what the rapid deterioration of the semiconductor material springs from, along with the resulting problems. In current scientific literature, the terms EGFET and SEGFET involve two different modes of approaching the development of electro–chemical biosensors for the detection of analytes.

In the years most of the efforts have been focused on the possibility to apply materials (often insulating materials) in the field of ion sensing, which actually establish well–defined design criteria, starting from more classic metal/metal oxides electrodes, to the more recent nanostructured materials, not neglecting the use of different material such as paper [27, 28, 36, 37, 100–104, 120–135, 136–138]. Although the literature reports different attempts to improve the performances of the EGFETs mainly acting on high aspect ratio, reducing leakage current, as well as parasitic capacitances, many devices are based on commercial FET as reported in Table 7 [139, 140]. The use of commercial devices has been often preferred because of the easier fabrication process and the lower cost.

Table 7. FET Devices Characteristics for EGFET Sensors

Ref.	FET device	Model	CMOS Process (μm)	Main features	W/L (μm)
[140]	NC	N/A	0.5	CMOS –DPDM n–well	600/20
[141, 142, 144, 146, 153–155, 157, 159]	C	CD4007UB	nr	CMOS dual complementary pair plus inverter	nr
[143, 145]	C	NDP6060L	nr	n–channel logic level enhancement mode FET	nr
[147, 158]	C	HEF4007	nr	Dual complementary pair and inverter	nr
[148]	C	BS170	nr	n–channel MOSFET	9700/2
[149]	NC	N/A	0.16	Differential source–follower	8/2
[150]	NC	N/A	0.35	Rectangular p–type MOSFET	18/1
[151]	NC	N/A	0.6	Pt and Au gate MOSFET	100/10
[152]	C	LT1167	nr	Instrumentation Amplifier	nr
[156]	C	2SK246Y	nr	n–channel junction FET	nr

C: Commercial FET device, NC: Non Commercial FET device. DPDM: Double Poly Double Metal. nr: not reported. N/A: not applicable.

As far as pH sensors are concerned, the sensitivity does not show significant changes in the reviewed literature, ranging from 45 mV/pH for ZnO nanorod layer [93], to 62.87 mV/pH of the most expensive PdO sensing element [100]. The problem of threshold voltage drift seems to represent still a bottleneck ranging from 0.04 mV/h [101] up to 13.2 mV/h [79]. On the other hand, the sensitivity of Urea and Glucose sensors based on EGFET is mostly affected by the sensitive layer leading to high range variability. There are many interesting applications and opportunities for the successful development of EGFET based biosensors, such as drug discovery, clinical diagnosis of diseases, biomedicine, food safety and processing, environmental monitoring, etc.. In particular, the development of disposable and portable detection systems is often preferred over the sensitive laboratory–based techniques. Interesting examples are continuous glucose monitoring in diabetic patients, remote sensing of airborne bacteria in counter–bioterrorist activities, routine analytical parameters. In addition, the detection of specific DNA sequences and the study of gene polymorphisms play a fundamental role in the rapid detection of genetic mutations and sequencing of the genome, offering the possibility of performing reliable diagnosis even before any symptoms of a disease appear. Apart from this positive note, very stringent laboratory standards, guidelines and regulations require that EGFET development should strongly fit with the specific demand. Increasing efforts in FET design could be a key point in order to make a significant contribution in the development of EGFET based chemical sensors, which could be one of the reasons for industry to invest in on more reliable chemical sensors.

Conflicts of Interest: The authors declare no conflict of interest.

References

1. Bergveld, P. Development of an Ion–Sensitive Solid–State Device for Neurophysiological Measurements. *IEEE Transactions on Biomedical Engineering* **1970**, *17*, 70–71, 10.1109/TBME.1970.4502688.
2. Luz, R.A.S.; Rodrigo, M.; Crespilho, I.; Crespilho, F.N. Nanomaterials for Biosensors and Implantable Biodevices. In *Nanobioelectrochemistry: From Implantable Biosensors to Green Power Generation*. Springer–Verlag: Berlin Heidelberg, 2013; pp. 27–8, 978–3–642–29249–1
3. Van der Spiegel, J.; Lauks, I.; Chan, P.; Babic, D. The extended gate chemically sensitive field effect transistor as multi–species microprobe. *Sensors and Actuators* **1983**, *4*, 291–298, 10.1016/0250–6874(83)85035–5.
4. Batista, P.D.; Mulato, M. ZnO extended–gate field–effect transistors as pH sensors. *Applied Physics Letters* **2005**, *87*, 143508. 10.1063/1.2084319.
5. Schöning, M.J.; Poghossian, A. Bio FEDs (Field–Effect Devices): state–of–the–art and new directions, *Electroanalysis* **2006**, 18, 1893–1900. 10.1002/elan.200603609.
6. Pijanowska, D.G.; Torbicz, W. pH–ISFET based urea biosensor. *Sensors Actuators B: Chemical* **1997**, *44*, 370–376. 10.1016/S0925–4005(97)00194–9.
7. Pan, T–M.; Huang, M–D.; Lin, C–W.; Wu, M–H. Development of high–κ $HoTiO_3$ sensing membrane for pH detection and glucose biosensing. *Sensors Actuators B: Chemical* **2010**, *144*, 139–145. 10.1016/j.snb.2009.10.049.
8. Lin, Y–H.; Wang, S–H.; Wu, M–H.; Pan, T–M.; Lai, C–S.; Luo, J–D.; Chiou, C–C. Integrating solid–state sensor and microfluidic devices for glucose, urea and creatinine detection based on enzyme–carrying alginate microbeads. *Biosensors and Bioelectronics* **2013**, *43*, 328–335. 10.1016/j.bios.2012.12.053.
9. Hideshima, S.; Sato, R.; Kuroiwa, S.; Osaka, T. Fabrication of stable antibody–modified field effect transistors using electrical activation of Schiff base cross–linkages for tumor marker detection. *Biosensors and Bioelectronics* **2011**, *26*, 2419–2425. 10.1016/j.bios.2010.10.023.
10. Selvanayagam, Z.E.; Neuzil, P.; Gopalakrishnakone, P.; Sridhar, U.; Singh, M.; Ho, L.C. An ISFET–based immunosensor for the detection of β–bungarotoxin. *Biosensors and Bioelectronics* **2002**, *17*, 821–826. 10.1016/S0956–5663(02)00075–1.
11. Fiorillo, A.S.; Van Der Spiegel, J.; Bloomfield, P.E.; Esmail–Zandi, D. A P(VDF–TrFE)–based Integrated Ultrasonic Transducer. *Sensors and Actuators A: Physical* **1990**, *22*, 719–725. 10.1016/0924–4247(89)80065–2.
12. Van der Spiegel, J.; Fiorillo, A.S. Method of manufacturing ferroelectric MOSFET sensors. *Patent US5254504A*, 1989.
13. Sung, M.; Shin, K,; Moon, W. A micro–machined hydrophone employing a piezoelectric body combined on the gate of a field–effect transistor. *Sensors and Actuators A: Physical* **2016**, *237*, 155–166. 10.1016/j.sna.2015.11.025.
14. Lambrechts, M.; Sansen, W. *Biosensors: Microelectrochemical devices*, Institute of Physics Publishing: Bristol, 1992, 978–0750301121.
15. Valdes Zaldivar, E.; Lastres Capote, A.; Horna, C.D.; Arias de Fuentes, O.; Estudio de la deriva del isfet utilizando instrumentaciòn virtual. XI IBERCHIP Workshop, Salvador de Bahía, Brasil, 28–30 March, 2005.
16. Poghossian, A.S.; Method of Fabrication of ISFETs and CHEMFETs on an Si–SiO2–Si Structure. *Sensors and Actuators B: Chemical* **1993**, *14*, 653–654. 10.1016/0925–4005(93)85130–3.
17. Codinachs, L.M.I.; Baldi, A.; Merlos, A.; Abramova, N.; Ipatov, A.; Jimenez–Jorquera, C.; Bratov, A. Integrated Multisensor for FIA–Based Electronic Tongue Applications. *IEEE Sensors Journal* **2008**, *8*, 608–615. 10.1109/JSEN.2008.918965.
18. Kimura, J.; Kuriyama, T.; Kawana, Y. An integrated SOS/FET multi–biosensor. *Sensors and Actuators* **1986**, *9*, 373–387. 10.1016/0250–6874(86)80069–5.
19. Cane, C.; Gracia, I.; Merlos, A. Microtechnologies for pH ISFET Chemical Sensors. *Microelectronics Journal* **1997**, *28*, 389–405. 10.1016/S0026–2692(96)00068–7.

20. Ho, N.J.; Kratochvil, J.; Blackburn, G.F.; Janata, J. Encapsulation of polymeric membrane–based ion–selective field effect transistor. *Sensors and Actuators* **1983**, *4*, 413–421. 10.1016/0250–6874(83)85052–5.
21. Van Der Schoot, B.H.; Van Den Vlekkert, H.H.; De Rooij, N.F.; Van Den Berg, A.; Grisel, A. A flow injection analysis system with glass–bonded ISFETs for the simultaneous detection of calcium and potassium ions and pH. *Sensors and Actuators B: Chemical* **1991**, *4*, 239–241. 10.1016/0250–6874(83)85052–5.
22. Van den Vlekkert, H.H.; de Rooij, N.F. Design, fabrication and characterization of pH sensitive isfets. *Analysis* **1988**, *16*, 2, 110.
23. Shinwari, W.M.; Zhitomirsky, D.; Deen, I.A.; Selvaganapathy, P.R.; Deen, M.J.; Landheer, D. Microfabricated reference electrodes and their biosensing applications. *Sensors* **2010**, *10*, 1679–1715. 10.3390/s100301679.
24. Lin, Y.H.; Chu, C.P.; Lin, C.F.; Liao, H.H.; Tsai, H.H.; Juang, Y.Z. Extended–gate field–effect transistor packed in micro channel for glucose, urea and protein biomarker detection. *Biomedical Microdevices* **2015**, *17*, 111. 10.1007/s10544–015–0020–4.
25. Magee, A. Fabrication and design of EGFET devices for biosensing. *NNIN REU Research Accomplishments*, Ithaca, USA, 9–12 Aug. 2015.
26. Kwon, I.; Lee, H–H.; Choi, J.; Shin, J–K.; Seo, S–H.; Choi, S–W.; Chun, H–S. Extended–Gate metal oxide semiconductor field effect transistor–based biosensor for detection of deoxynivalenol. *Japanese Journal of Applied Physics* **2011**, *50*, 06GL08. 10.7567/JJAP.50.06GL08.
27. Yin, L.T.; Chou, J.C.; Chung, W.Y.; Sun, T.P.; Hsiung, S.K. Study of indium tin oxide thin film for separative extended gate ISFET. *Material Chemistry and Physics* **2001**, *70*, 12–16. 10.1016/S0254–0584(00)00373–4.
28. Chi, L–L; Chou J–C; Chung, W–Y; Sun, T–P; Hsiung, S–K. Study on extended gate field effect transistor with tin oxide sensing membrane. *Materials Chemistry and Physics* **2000**, *63*, 19–23. 10.1016/S0254–0584(99)00184–4.
29. Brouk, I.; Nemirovsky, Y. l/f noise in CMOS transistors for analog applications. 21st IEEE Convention of the Electrical and Electronic Engineers in Israel, Tel–Aviv, Israel, 11–12 April, 2001.
30. Francis, S.A.; Dasgupta, A.; Fleetwood, D.M. Effects of total dose irradiation on the gate–voltage dependence of the 1/f noise of nMOS and pMOS transistors. *IEEE Transactions on Electron Devices* **2010**, 57, 503–510. 10.1109/TED.2009.2036297.
31. Tedja, S.; Van Der Spiegel, J.; Williams, H.H. Analytical and Experimental Studies of Thermal Noise in MOSFET's. *IEEE Transactions on Electron Devices* **1994**, *41*, 2069–2075. 10.1109/16.333824.
32. Kaisti, M.; Alexandrovna Boeva, Z.; Koskinen, J.; Nieminen, S.; Bobacka, J.; Levon, K. Hand–held transistor based electrical and multiplexed chemical sensing system. *ACS Sensors* **2016**, *1*, 1423–1431. 10.1021/acssensors.6b00520.
33. Brews, J.R.; Fichtner, W.; Nicollian, E.H.; Sze, S.M. Generalized guide for MOSFET miniaturization. *IEEE Electron Device Letters* **1980**, *1*, 2–4. 10.1109/EDL.1980.25205.
34. Chi, Y.; Maier, C.; Cauwenberghs, G. Ultra–high input impedance, low noise integrated amplifier for noncontact biopotential sensing. *IEEE Trans. Emerg. Sel. Topics Circuits Syst.* **2011**, *1*, 526–535. 10.1109/JETCAS.2011.2179419.
35. Poghossian, A.; Yoshinobu, T.; Simonis, A.; Ecken, H.; Luth, H.; Schoning, M.J. Penicillin detection by means of field–effect based sensors: EnFET, capacitive EIS sensor or LAPS?. *Sensors and Actuators B: Chemical* **2001**, *78*, 237–242. 10.1016/S0925–4005(01)00819–X.
36. Yusof, K.A.; Rahman, R.A.; Zulkefle, M.A.; Herman, S.H., Abdullah, W.F.H. EGFET pH sensor performance dependence on sputtered TiO2 sensing membrane deposition temperature, *Journal of Sensors* **2016**, 2016. 10.1155/2016/7594531.
37. Guerra, E.M.; Ribeiro Silva, G.; Mulato, M. Extended gate field effect transistor using V2O5 xerogel sensing membrane by sol–gel method. Solid State Sciences 2009, 11, 456–460. 10.1016/j.solidstatesciences.2008.07.014.
38. Ho, C.; Yu, H.–Z.; Aptamer–based electrochemical biosensors for the detection of small molecules and plasma proteins. In Microelectrode Biosensors. Neuromethods, Marinesco S., Dale N.; Humana Press, Totowa, NJ; 2013; 80, 319–346.

39. Karadurmus, L.; Kurbanoglu, S.; Uslu, B.; Ozkan, S.A. Electrochemical DNA biosensors in drug analysis. Current Pharmaceutical Analysis 2016, 12, 1–1. 10.2174/1573412912666160422152634.
40. Plumeré, N.; Henig, J.; Campbell, W.H. Enzyme–catalyzed O2 removal system for electrochemical analysis under ambient air: Application in an amperometric nitrate biosensor. *Analytical Chemistry* **2012**, *84*, 2141–2146. 10.1021/ac2020883.
41. Cizek, K.; Prior, C.; Thammakhet, C.; Galik, M.; Linker, K.; Tsui, R.; Cagan, A.; Wake, J.; La Belle, J.; Wang, J. Integrated explosive preconcentrator and electrochemical detection system for 2,4,6–trinitrotoluene (TNT) vapor. *Analytical Chimica Acta* **2010**, *66*, 117–121. 10.1016/j.aca.2009.12.008.
42. Zeng, Y.; Zhu, Z.; Du, D.; Lin, Y. Nanomaterial–based electrochemical biosensors for food safety. *Journal of Electroanalytical Chemistry* **2016**, *781*, 147–154. 10.1016/j.jelechem.2016.10.030.
43. Bratov, A.; Abramova, N.; Ipatov, A. Recent trends in potentiometric sensor arrays–A review. *Analytica Chimica Acta* **2010**, 678, 149–159. 10.1016/j.aca.2010.08.035.
44. Adibi, M.; Pirali–Hamedani, M.; Norouzi, P. Copper nano–composite potentiometric sensor. *International Journal of Electrochemical Science* **2011**, *6*, 717–726. 10.1007/s13738–014–0406–x
45. Zhang, Q.; Majumdar, H.S.; Kaisti, M.; Prabhu, A.; Ivaska, A.; Österbacka, R.; Rahman, A.; Levon, K. Surface functionalization of ion–sensitive floating–gate field effect transistors with organic electronics. *IEEE Transaction on Electron Devices* **2015**, *62*, 1291–1298. 10.1109/TED.2015.2396996.
46. Guan, W.; Rajan, N.K.; Duan, X.; Reed, M.A. Quantitative probing of surface charges at dielectric–electrolyte interfaces. *Lab on Chip* **2015**, *13*, 1431–1436. 10.1039/C3LC41351A.
47. Song, M.J.; Hwang, S.W.; Whang, D. Amperometric hydrogen peroxide biosensor based on a modified gold electrode with silver nanowires. *Journal of Applied Electrochemistry* **2010**, *40*, 2099–2105. 10.1007/s10800–010–0191–x.
48. Yang, P.; Wang, L.; Wu, Q.; Chen, Z.; Lin, X. A method for determination of glucose by an amperometric bienzyme biosensor based on silver nanocubes modified Au electrode, *Sensors and Actuator B: Chemical* **2014**, *194*, 71–78. 10.1016/j.snb.2013.12.074.
49. Adeloju, S. B.; Hussain, S. Potentiometric sulfite biosensor based on entrapment of sulfite oxidase in a polypyrrole film on a platinum electrode modified with platinum nanoparticles. *Microchimica Acta* **2016**, *183*, 1341–1350. 10.1007/s00604–016–1748–0.
50. Pal, R.K.; Kundu, S.C.; Yadavalli, V.K. Biosensing using photolithographically micropatterned electrodes of PEDOT:PSS on ITO substrates. *Sensors and Actuators B: Chemical* **2017**, *242*, 140–147. 10.1016/j.snb.2016.11.049.
51. Chauhan, N.; Rawal, R.; Hooda, V.; Jain, U. Electrochemical biosensor with graphene oxide nanoparticles and polypyrrole interface for the detection of bilirubin, *RSC Advances* **2016**, *6*, 63624–63633. 10.1039/C6RA15671A.
52. Sharma, A.; Kumar, A. Study of structural and electro–catalytic behaviour of amperometric biosensor based on chitosan/polypyrrole nanotubes–gold nanoparticles nanocomposites. *Synthetic Metals* 2016, *220*, 551–559. 10.1016/j.synthmet.2016.07.012.
53. Lin, J.; He, C.; Zhao, Y.; Zhang, S. One–step synthesis of silver nanoparticles/carbon nanotubes/chitosan film and its application in glucose biosensor. *Sensors and Actuators B: Chemicals* **2009**, *137*, 768–773. 10.1016/j.snb.2009.01.033
54. Shi, K.; Shiu, K.K. Scanning tunneling microscopic and voltammetric studies of the surface structures of an electrochemically activated glassy carbon electrode. *Analytical Chemistry* **2002**, *74*, 879–885. 10.1021/ac010734+.
55. Song, M.J.; Kim, J.H.; Lee, S.K.; Lim, D.S.; Hwang, S.W.; Whang, D. Analytical characteristics of electrochemical biosensor using pt–dispersed graphene on boron doped diamond electrode. *Electroanalysis* **2011**, *23*, 2408–2414. 10.1002/elan.201100265.
56. Zehani, N.; Fortgang, P.; Saddek Lachgar, M.; Baraket, A.; Arab, M.; Dzyadevych, S.V.; Kherrat, R.; Jaffrezic–Renault, N. Highly sensitive electrochemical biosensor for bisphenol A detection based on a diazonium–functionalized boron doped diamond electrode modified with a multi–walled carbon nanotube–tyrosinase hybrid film. *Biosensors and Bioelectronics* **2015,** *74*, 830–835. 10.1016/j.bios.2015.07.051.
57. Palanisamy, S.; Karuppiah, C.; Chen, S.M.; Periakaruppan, P. A highly sensitive and selective enzymatic biosensor based on direct electrochemistry of hemoglobin at zinc oxide nanoparticles

592 modified activated screen printed carbon electrod. *Electroanalysis* **2014**, *26*, 1984–1993.
593 10.1002/elan.201400304.
594 58. Al Mamun, K.A.; Islam, S.K.; Hensley, D.K.; McFarlane, N. A glucose biosensor using CMOS
595 potentiostat and vertically aligned carbon nanofibers, *IEEE Transactions on Biomedical Circuits and*
596 *Systems* **2016**, *10*, 807–816. 10.1109/TBCAS.2016.2557787.
597 59. Yu, Y.; Al Mamun, K.A.; Shanta, A.S.; Islam, S.K.; McFarlane, N. Vertically aligned carbon nanofibers
598 as a cell impedance sensor. *IEEE Transactions on Nanotechnology* **2016**, *15*, 856–861.
599 10.1109/TNANO.2016.2558102.
600 60. Islam, A.B., Islam, S.K.; Rahman, T. A highly selective mediator less glucose detector employing
601 vertically aligned carbon nanofiber (VACNF). *Sensors, 2010 IEEE*, Kona, HI, 1–4 Nov, 2010.
602 10.1109/ICSENS.2010.5690976.
603 61. Al Mamun, K.A.; Gu, J.; Hensley, D.K.; Islam, S.K.; McFarlane, N. Integration of carbon
604 nanostructures on CMOS for lab–on–a–chip sensing, 2016 IEEE International Symposium on Circuits
605 and Systems (ISCAS), Montreal, QC, 22–25 May 2016. 2879–2882. 10.1109/ISCAS.2016.7539194.
606 62. Islam, S.K.; Mahbub, I.; Shamsir, S.; Carbon nanomaterial based sensors for astrobiology exploration.
607 *2017 IEEE 60th International Midwest Symposium on Circuits and Systems (MWSCAS)*, Boston, MA, 6–9
608 Aug. 2017. 10.1109/MWSCAS.2017.8053219
609 63. Li, Y.; Li, Y.; Yang, Y. A new amperometric H_2O_2 biosensor based on nanocomposite films of
610 chitosan–MWNTs, hemoglobin, and silver nanoparticles. *Journal of Solid State Electrochemistry* **2012**, *16*,
611 1133–1140. 10.1007/s10008–011–1503–8.
612 64. Fang, Y.; Guo, S.; Zhu, C.; Zhai, Y.; Wang, E. Self–assembly of cationic polyelectrolyte–functionalized
613 graphene nanosheets and gold nanoparticles: A two–dimensional heterostructure for hydrogen
614 peroxide sensing. *Langmuir* **2010**, *26*, 11277–11282. 10.1021/la100575g.
615 65. Piao, Y.; Han, D.J.; Seo, T.S. Highly conductive graphite nanoparticle based enzyme biosensor for
616 electrochemical glucose detection. *Sensors and Actuators B: Chemical* **2014**, *194*, 454–459.
617 10.1016/j.snb.2013.12.045.
618 66. Wang, J.; Musameh, M.; Lin, Y. Solubilization of carbon nanotubes by Nafion toward the preparation
619 of amperometric biosensors. *Journal of the American Chemical Society* **2003**, *125*, 2408–2409.
620 10.1021/ja028951v.
621 67. Braik, M.; Barsan, M.M.; Dridi, C.; Ben Ali, M.; Brett, C.M.A. Highly sensitive amperometric enzyme
622 biosensor for detection of superoxide based on conducting polymer/CNT modified electrodes and
623 superoxide dismutase. *Sensors and Actuators B: Chemical* **2016**, *236*, 574–582. /10.1016/j.snb.2016.06.032.
624 68. Malhotra, B.D.; Chaubey, A. Biosensors for clinical diagnostics industry. *Sensors and Actuators B:*
625 *Chemical* **2003**, *91*, 117–127. 10.1016/S0925–4005(03)00075–3.
626 69. Harguindey, S.; Pedraz, J.L.; Garcia Canero, R.; Perez de Diego, J.; Cragoe. E.J. Hydrogen
627 ion–dependent oncogenesis and parallel new avenues to cancer prevention and treatment using a
628 H(+)–mediated unifying approach: pH–related and pH–unrelated mechanisms. *Critical Reviews in*
629 *Oncogenesis* **1995**, *6*, 1–33.
630 70. Gottlieb, R.A.; Dosanjh. A. Mutant cystic fibrosis transmembrane conductance regulator inhibits
631 acidification and apoptosis in C127 cells: possible relevance to cystic fibrosis, *PNAS* **1996**, *6*,
632 3587–3591.
633 71. Miksa, M.; Komura, H.; Wu, R.; Shah, K.G.; Wang, P. A novel method to determine the engulfment of
634 apoptotic cells by macrophages using phrodo succinimidyl ester. *Journal of Immunological Methods*
635 **2009**, *342*, 71–77. 10.1016/j.jim.2008.11.019.
636 72. Lakadamyali, M.; Rust, M.J.; Babcock, H.P.; Zhuang, X. Visualizing infection of individual influenza
637 viruses, *PNAS* **2013**, *100*, 9280–9285. 10.1073/pnas.0832269100.
638 73. Fog, A.; Buck, R.P. Electronic semiconducting oxides as pH sensors, *Sensors and Actuators* **1984**, *5*,
639 137–146. 10.1016/0250–6874(84)80004–9.
640 74. Al–Hardan, N.H.; Hamid, M.A.A.; Ahmed, N.M.; Jalar, A.; Shamsudin, R.; Othman, N.K.; Keng, L.K.;
641 Chiu, W.; Al–Rawi, H.N. High sensitivity pH sensor based on porous silicon (PSi) extended gate
642 field–effect transistor. *Sensors* **2016**, 16 , 839. 10.3390/s16060839.

643 75. Sabah, F.A.; Ahmed, N.M.; Hassan, Z.; Almessiere, M.A.; Al–hardan, N.H. Sensitivity of CuS
644 membrane pH sensor with and without MOSFET, *JOM* **2017**, *69*, 1134–1142.
645 10.1007/s11837–016–2165–x.
646 76. Banna, M.H.; Najjaran, H.; Sadiq, R.; Imran, S.A.; Rodriguez, M.J.; Hoorfar, M. Miniaturized Water
647 Quality Monitoring pH and Conductivity Sensors. *Sensors and Actuators B: Chemical* **2014**, *193*, 434–441.
648 10.1016/j.snb.2013.12.002.
649 77. Bohnke, C.; Duroy, H.; Fourquet, J.–L. pH sensors with lithium lanthanum titanate sensitive material:
650 Applications in food industry. *Sensors and Actuators B: Chemical* **2003**, *89*, 240–247.
651 10.1016/S0925–4005(02)0047322.
652 78. Kwon, D–H.; Cho, B–W.; Kim, C–S.; Sohn, B–K. Effects of heat treatment on Ta_2O_5 sensing membrane
653 for low drift and high sensitivity pH–ISFET. *Sensors and Actuators B: Chemical* **1996**, *34*, 441–445.
654 10.1016/S0925–4005(96)01938–7.
655 79. Lue, C–E; Wang, I–S; Huang, C–H; Shiao, Y–T; Wang, H–C; Yang, C–M; Hsu, S.H.; Chang, C.Y.;
656 Wang, W.; Lai, C.S. pH sensing reliability of flexible ITO/PET electrodes on EGFETs prepared by a
657 roll–to–roll process. *Microelectronics Reliability* **2012**, *52*, 1651–1654. 10.1016/j.microrel.2011.10.026.
658 80. Vieira, N.C.S.; Fernandes, E.G.R.; de Queiroz, A.A.A.; Guimarães, F.E.G.; Zucolotto, V. Indium tin
659 oxide synthesized by a low cost route as SEGFET pH sensor. *Material Research* **2013**, *16*, 1156–1160.
660 10.1590/S1516–14392013005000101.
661 81. Yang, C–M .; Wang, I–S.; Lin, Y–T.; Huang, C–H.; Lu, T–F.; Lue, C–E.; Pijanowska, D.G.; Hua, M–Y.;
662 Lai, C–S. Low cost and flexible electrodes with NH_3 plasma treatments in extended gate field effect
663 transistors for urea detection, *Sensors and Actuators B: Chemical* **2013**, *187*, 274–279.
664 10.1016/j.snb.2012.11.023.
665 82. Chen, J–C.; Chou, J–C.; Sun, T–P.; Hsiung, S–K. Portable urea biosensor based on the extended–gate
666 field effect transistor sensor, *Sensors and Actuators B: Chemical* **2003**, *91*, 180–186.
667 10.1016/S0925–4005(03)00161–8.
668 83. Pan, C–W.; Chou, J–C.; Sun, T–P.; Hsiung, S–K. Development of the tin oxide pH electrode by the
669 sputtering method, *Sensors and Actuators B: Chemical* **2005**, *108:1–2*, 863–869. 10.1016/j.snb.2004.11.033.
670 84. Nguyen, T.N.T.; Seol, Y.G.; Lee, N–E. Organic field–effect transistor with extended indium tin oxide
671 gate structure for selective pH sensing, *Organic Electronics* **2011**, *12:11*, 1815–1821.
672 10.1016/j.orgel.2011.07.009.
673 85. Kao, C–H.; Chen, H.; Kuo, L–T.; Wang, J–C.; Chen, Y–T.; Chu, Y–C.; Chen, C–Y.; Lai, C–S.; Chang,
674 S.W.; Chang, C.W. Multi–analyte biosensors on a CF_4 plasma treated Nb_2O_5–based membrane with an
675 extended gate field effect transistor structure, *Sensors Actuators B: Chemical* **2014**, *194*, 419–426.
676 10.1016/j.snb.2013.12.056.
677 86. Asif, M.H.; Nur, O.; Willander, M.; Danielsson, B. Selective calcium ion detection with functionalized
678 ZnO nanorods–extended gate MOSFET, *Biosensors and Bioelectronics* **2009**, *24*, 3379–3382.
679 10.1016/j.bios.2009.04.011.
680 87. Fathil, M.F.M.; Arshad Md, M.K.; Ruslinda, A.R.; Gopinath, S.C.B.; Nuzaihan Md Nor, M.; Adzhri, R.;
681 Hashim, U.; Lam, H.Y. Substrate–gate coupling in ZnO–FET biosensor for cardiac troponin I
682 detection, *Sensors and Actuators B: Chemical* **2017**, *242*, 1142–1154. 10.1016/j.snb.2016.09.131.
683 88. Wang, J–L.; Yang, P–Y.; Hsieh, T–Y.; Juan, P–C. Ionic pH and glucose sensors fabricated using
684 hydrothermal ZnO nanostructures, *Japanese Journal of Applied Physics* **2015**, *55:1S*, 01AE16.
685 10.7567/JJAP.55.01AE16.
686 89. Liao, Y–H.; Chou, J–C. Preparation and characterization of the titanium dioxide thin films used for pH
687 electrode and procaine drug sensor by sol–gel method, *Materials Chemistry and Physics* **2009**, *114:2–3*,
688 542–548. 10.1016/j.matchemphys.2008.10.014.
689 90. Chou, J.C.; Tzeng, D.J. Study on the characteristics of the ruthenium oxide pH electrode, *Rare Metal*
690 *Materials and Engineering* **2006**, *35*, 603–612. 10.1016/j.snb.2007.07.023.
691 91. Wu, Y–C.; Wu, S–J.; Lin, C–H. High performance EGFET–based pH sensor utilizing low–cost
692 industrial–grade touch panel film as the gate structure, *IEEE Sensors Journal* **2015**, *15:11*, 6279–6286.
693 10.1109/JSEN.2015.2455057.

92. Tsai, C–N.; Chou, J–C.; Sun, T–P.; Hsiung, S–K. Study on the sensing characteristics and hysteresis effect of the tin oxide pH electrode, *Sensors and Actuators B: Chemical* **2005**, *108*, 877–882. 10.1016/j.snb.2004.11.050.
93. Qi, J.; Zhang, H.; Ji, Z.; Xu, M.; Zhang, Y. ZnO nano–array–based EGFET biosensor for glucose detection, *Applied Physics A* **2015**, *119:3*, 807–811. 10.1007/s00339–015–9122–3.
94. Wang, J–L.; Yang, P–Y.; Hsieh, T–Y.; Hwang, C–C.; Juang, M–H. pH–sensing characteristics of hydrothermal Al–doped ZnO nanostructures, *Journal of Nanomaterials* **2013**, *2013*, 1–7. 10.1155/2013/152079.
95. Chou, J–C.; Wang, Y.S. Biosensor, method of manufacturing sensing unit thereof, and measuring system, US Patent, *20040256685A1*, **2004**.
96. Yin, L–T.; Wang, H–Y.; Lin, Y–C.; Huang, W–C. A novel instrumentation circuit for electrochemical measurements, *Sensors* **2012**, *12:7*, 9687–9696. 10.3390/s120709687.
97. Sun, C.; Zeng, R.; Zhang, J.; Qiu, Z–J.; Wu, D. Effects of UV–ozone treatment on sensing behaviors of EGFETs with Al_2O_3 sensing film, *Materials* **2017**, *10*, 1–11. 10.3390/ma10121432.
98. Tarasov, A.; Wipf, M.; Stoop, R.L.; Bedner, K.; Fu, W.; Guzenko, V.A.; Knopfmacher, O.; Calame, M.; Schönenberger, C. Understanding the electrolyte background for biochemical sensing with ion–sensitive field–effect transistors, *ACS Nano* **2012**, *6*, 9291–9298. 10.1021/nn303795r.
99. Van Hal, R.E.G.; Eijkel, J.C.T.; Bergveld, P. A novel description of ISFET sensitivity with the buffer capacity and double–layer capacitance as key parameters, *Sensors and Actuators B: Chemical* **1995**, *24*, 201–205. 10.1016/0925–4005(95)85043–0.
100. Das, A.; Ko, D.H.; Chen, C–H.; Chang, L–B.; Lai, C–S.; Chu, F–C.; Chow, L.; Lin, R–M. Highly sensitive palladium oxide thin film extended gate FETs as pH sensor, *Sensors and Actuators B: Chemical* **2014**, *205*, 199–205. 10.1016/j.snb.2014.08.057.
101. Yang, C–M.; Wang, J–C.; Chiang, T–W.; Lin, Y–T.; Juan, T–W.; Chen, T–C.; Shih, M–Y.; Lue, C–E.; Lai, C–S. Hydrogen ion sensing characteristics of IGZO/Si electrode in EGFET, *International Journal of Nanotechnology* **2014**, *11*, 1–4. 10.1504/IJNT.2014.059806.
102. Batista, P.D. An embedded measurement system for electrical characterization of EGFET as pH sensor, *Measurement Science and Technology* **2013**, *25:2*. 10.1088/0957–0233/25/2/027001.
103. Chien, Y–S.; Tsai, W–L.; Lee, I–C.; Chou, J–C.; Cheng, H–C. A novel pH sensor of extended–gate field–effect transistors with laser–irradiated carbon–nanotube network, *IEEE Electron Device Letters* **2012**, *33:11*, 1622–1624. 10.1109/LED.2012.2213794.
104. Silva, G.O.; Mulato, M. Urea–EnFET biosensor based on pHEGFET using FTO and ITO support films, *223rd ECS Meeting*, Toronto, Canada, May 12–16, 2013.
105. Lue, C–E.; Yu, T–C.; Yang, C–M.; Pijanowska, D.G.; Lai, C–S. Optimization of urea– EnFET based on Ta_2O_5 layer with post annealing, *Sensors* **2011**, *11*, 4526–4571. 10.3390/s110504562.
106. Chiu, Y–S.; Tseng, C–Y.; Lee, C–T. An extended–gate CMOS sensor array with enzyme–immobilized microbeads for redox–potential glucose detection, *Biomedical Circuits and Systems Conference (BioCAS)*, Lausanne, Switzerland, 2014.
107. Chirizzi, D.; Malitesta, C. Potentiometric urea biosensor based on urease immobilized by an electrosynthesized poly(o–phenylenediamine) film with buffering capability, *Sensors and Actuators B Chemical* **2011**, *157:1*, 211–215. 10.1016/j.snb.2011.03.051.
108. Temple–Boyer, P.; Benyahia, A.; Sant, W.; Pourciel–Gouzy, M.L.; Launay, J. A. Martinez, Modelling of urea–EnFETs for haemodialysis applications, *Sensors and Actuators B: Chemical* **2008**, *131*, 525–532. 10.1016/j.snb.2007.12.037.
109. Sun, L–P.; Zhang, Z.; Wang, S.; Zhang, J.; Li, H.; Ren, L.; Weng, J.; Zhang, Q. Effect of pH on the interaction of gold nanoparticles with DNA and application in the detection of human p53 gene mutation, *Nanoscale Research Letters* **2009**, **4**, 216–220. 10.1007/s11671–008–9228–z.
110. Prakash, O.; Puliga, S.; Upadhyay, L.S.B. Immobilization of watermelon (citrullus vulgaris) urease in agarose gel for urea estimation, *Biotechnology Bioprocess Engineering* **2007**, *12*, 131–135. 10.1007/BF03028638.
111. Dhawan, G.; Sumana, G.; Malhotra, B.D. Recent developments in urea biosensors, *Biochemical Engineering Journal* **2009**, *44*, 42–52. 10.1016/j.bej.2008.07.004.

112. Sungur, S.; Murat Elcin, Y.; Akbulut, U. Studies on immobilization of urease in gelatin by cross–linking, *Biomaterials*, 13:11 (2003) 795–800. 10.1016/0142–9612(92)90020–O.
113. Yin, L–T.; Lin, Y–T.; Leu, Y–C.; Hu, C–Y. Enzyme immobilization on nitrocellulose film for pH–EGFET type biosensors, *Sensors and Actuators B: Chemical* **2010**, *148*, 207–213. 10.1016/j.snb.2010.04.042.
114. Siqueira, J.R.; Fernandes, E.G.R.; de Oliveira, O.N.; Zucolotto, V. Biosensors Based on Field–Effect Devices. In: Crespilho F. (eds) Nanobioelectrochemistry. Springer, Berlin, Heidelberg, 2013. 10.1007/978–3–642–29250–7_4.
115. Clark Jr., L.C.; Lyons, C. Electrode systems for continuous monitoring in cardiovascular surgery, *Annals of the New York Academy of Sciences* **1962**, *102*, 29–45. 10.1111/j.1749–6632.1962.tb13623.x.
116. Lei, Y.; Yan, X.; Zhao, J.; Liu, X.; Song, Y.; Luo, N.; Zhang, Y. Improved glucose electrochemical biosensor by appropriate immobilization of nano–ZnO, *Colloids and Surfaces B: Biointerfaces* **2011**, *82:1*, 168–172. 10.1016/j.colsurfb.2010.08.034.
117. Yang, K.; She, G–W.; Wang, H.; Ou, X–M.; Zhang, X–H.; Lee, C–S.; Lee, S–T. ZnO Nanotube arrays as biosensors for glucose, *Journal of Physical Chemistry C* **2009**, *113*, 20169–20172. 10.1021/jp901894j
118. Zhao, Y.; Yan, X.; Kang, Z.; Lin, P.; Fang, X.; Lei, Y.; Ma, S.; Zhang, Y. Highly sensitive uric acid biosensor based on individual zinc oxide micro/nanowires, *Microchimica Acta* **2013**, *180:9–10*, 759–766. 10.1007/s00604–013–0981–z.
119. Umar, A.; Rahman, M.M.; Kim, S.H.; Hahn, Y.B. ZnO nanonails: synthesis and their application as glucose biosensor, *Journal of Nanoscience and Nanotechnology* **2008**, *8:6*, 3216–3221.
120. Vieira, N.C.S.; Figueiredo, A.; de Queiroz, A.A.A.; Zucolotto, V.; Guimarães, F.E.G. Self–Assembled Films of Dendrimers and Metallophthalocyanines as FET–Based Glucose Biosensors, *Sensors* **2011**, *11*, 9442–9449. 10.3390/s111009442.
121. Anan, H.; Kamahori, M.; Ishige, Y.; Nakazato, K. Redox–potential sensor array based on extended–gate field–effect transistors with ω–ferrocenylalkanethiol–modified gold electrodes, *Sensors and Actuators B: Chemical* **2013**, *187*, 254–261. 10.1016/j.snb.2012.11.016.
122. Chou, J–C.; Yang, H–Y.; Chen, C–W. Glucose biosensor of ruthenium–doped TiO_2 sensing electrode by co–sputtering system, *Microelectronics Reliability* **2010**, 50, 753–756. 10.1016/j.microrel.2010.01.025.
123. Lee, C–T.; Chiu, Y–S.; Ho, S–C.; Lee, Y–J. Investigation of a photoelectrochemical passivated ZnO–based glucose biosensor, *Sensors* **2011**, *11*, 4648–4655. 10.3390/s110504648.
124. Fathollahzadeh, M.; Hosseini, M.; Norouzi, M.; Ebrahimi, A.; Fathipour, M.; Kolahdouz, M.; Haghighi, B. Immobilization of glucose oxidase on ZnO nanorods decorated electrolyte–gated field effect transistor for glucose detection, *Journal of Solid State Electrochemistry* **2018**, *22:1*, 61–67. 10.1007/s10008–017–3716–y.
125. Riccardi, D.; Valenti, G. Localization and function of the renal calcium–sensing receptor, *Nature Reviews Nephrology* **2016**, *12*, 414–425. 10.1038/nrneph.2016.59.
126. Pinton, P.; Giorgi, C.; Siviero, R.; Zecchini, E.; Rizzuto, R. Calcium and apoptosis: ER–mitochondria Ca^{2+} transfer in the control of apoptosis, *Oncogene* **2008**, *27:50*, 6407–6418. 10.1038/onc.2008.308.
127. Vieira, N.C.S.; Figueiredo, A.; Faceto, A.D.; de Queiroz, A.A.A.; Zucolotto, V.; Guimarães, F.E.G. Dendrimers/TiO_2 nanoparticles layer–by–layer films as extended gate FET for pH detection, *Sensors and Actuators B: Chemical* **2012**, *169:5*, 397–400. 10.1016/j.snb.2012.01.003.
128. Sardarinejad, A.; Maurya, D.; Alameh, K. The pH Sensing Properties of RF Sputtered RuO_2 Thin–Film Prepared Using Different Ar/O_2 Flow Ratio, *Materials* **2015**, *8*, 3352–3363. 10.3390/ma8063352.
129. Rasheed, H.S.; Ahmed, N.M.; Matjafri, M.Z.; Al–Hardan, N.H.; Almessiere, M.A.; Sabah, F.A.; Al–Hazeem, N.Z. Multilayer ZnO/Pd/ZnO structure as sensing membrane for extended–gate field–effect transistor (EGFET) with high pH sensitivity, *Journal of Electronic Materials* **2017**, *46:10*, 5901–5908. 10.1007/s11664–017–5580–z.
130. Chou, J–C.; Sung, H–F.; Hsia, W–L.; Huang, Y–P. Calcium ion sensors and fabrication method thereof, and sensing systems comprising the same, US20090266712A1, **2009**.
131. Chou, J–C.; Chen, C–W.; Jiang, Y–H. Method for forming extended gate field effect transistor (EGFET) based sensor and the sensor therefrom, US Patent US20090278175 A1, **2012**.
132. Chung, W–Y.; Silverio, A.A.; Tsai, V.F.S.; Cheng, C.; Chang, S–Y.; Ming–Ying, Z.; Kaoc, C–Y.; Chend, S–Y.; Pijanowska, D. An implementation of an electronic tongue system based on a multi–sensor

potentiometric readout circuit with embedded calibration and temperature compensation, *IEEE Sensors Conference*, Busan, South Korea, 1–4 Nov. 2015.

133. Asif, M.H.; Nur, O.; Willander, M.; Yakovleva, M.; Danielsson, B. Studies on calcium ion selectivity of ZnO nanowire sensors using ionophore membrane coatings, *Research Letters in Nanotechnology* **2008**, *2008*, 1–4. 10.1155/2008/701813
134. Purwidyantri, A.; Kamajaya, L.; Chen, C–H.; Luo, J–D.; Chiou, C–C.; Tian, Y–C.; Lin, C–Y.; Yang, C–M.; Lai, C–S. A colloidal nanopatterning and downscaling of a highly periodic Au nanoporous EGFET biosensor, *Journal of the Electrochemical Society* **2018**, *165:4*, 3170–3177. 10.1149/2.0241804jes.
135. Chen, C–P.; Ganguly, A.; Lu, C–Y.; Chen, T–Y.; Kuo, C–C.; Chen, R–S.; Tu, W–H.; Fischer, W.B.; Chen, K–H.; Chen, L–C. Ultrasensitive in situ label–free DNA detection using a GaN nanowire–based extended–gate field–effect–transistor sensor, *Analytical Chemistry* **2011**, *83:6*, 1938–1943. 10.1021/ac102489y
136. Vieira, N.C.S.; Figueiredo, A.; dos Santos, J.F.; Aoki, S.M.; Guimarãesb, F.E.G.; Zucolotto, V. Label–free electrical recognition of a dengue virus protein using the SEGFET simplified measurement system, *Analytical Methods* **2014**, *6:22*, 8882–8885. 10.1039/C4AY01803F.
137. Sakata, T.; Matsumoto, S.; Nakajima, Y.; Miyahara, Y. Potential behavior of biochemically modified gold electrode for extended–gate field–effect transistor, *Japanese Journal of Applied Physics* **2005**, 44:4S. 10.1143/JJAP.44.2860.
138. Kim, D.; Park, J.; Shin, J.; Kim, P.K.; Lim, G.; Shoji, S. An extended gate FET–based biosensor integrated with a Si microfluidic channel for detection of protein complexes, *Sensors and Actuators B: Chemical* **2006**, *117:2*, 488–494. 10.1016/j.snb.2006.01.018.
139. Cho, W.; Lim, C. Sensing properties of separative paper–based extended–gate ion–sensitive field–effect transistor for cost effective pH sensor applications, *Solid–State Electronics* **2017**, *140*, 96–99. 10.1016/j.sse.2017.10.025.
140. Park, J.; Cho, W. Development of high–performance fully depleted silicon–on–insulator based extended–gate field–effect transistor using the parasitic bipolar junction transistor effect, *Applied Physics Letters* **2012**, *101:13*, 133703. 10.1063/1.4757000
141. Chin, Y.; Chou, J.; Lei, Z.; Sun, T.; Chung, W.; Hsiung, S. Titanium nitride membrane application to extended gate field effect transistor pH sensor using VLSI technology, *Japanese Journal of Applied Physics* **2001**, 40:11R, 6311. 10.1143/JJAP.40.6311.
142. Fernandes, E.G.R.; Vieira, N.C.S.; de Queiroz, A.A.A.; Guimarães, F.E.G.; Zucolotto, V. Immobilization of poly(propylene imine) dendrimer/nickel phtalocyanine as nanostructured multilayer Films to be used as gate membranes for SEGFET pH sensors, *Journal of Physical Chemistry C* **2010**, *114*, 6478–6483. 10.1021/jp9106052.
143. Purwidyantri, A.; Lai, H–C.; Tsai, S–H.; Luo, J–D.; Chioud, C–C.; Tiane, Y–C.; Cheng, C–H.; Linf, Y–T.; Laif, C–S. Sensing performance of fibronectin–functionalized Au–EGFET on the detection of S. epidermidis biofilm and 16S rRNA of infection–related bacteria in peritoneal dialysis, *Sensors and Actuators B: Chemical* **2015**, *217*, 92–99. 10.1016/j.snb.2014.11.017.
144. Zulkefle, M.A.; Rahman, R.A.; Mahmood, M.R.; Abdullah, W.F.H.; Herman, S.H. Sensing capability of TiO2 thin films with different thicknesses as sensing membrane of EGFET pH sensor, *International Symposium on Technology Management and Emerging Technologies (ISTMET)*, Langkawai Island, Malaysia, 25–27 Aug. 2015
145. Lin, F.; Chang, H.Y.; Hsiao, S.H.; Chen, H.I.; Liu, W.C. Preparation and characterization of nickel oxide–based EGFET pH sensors, *9th International Conference on Sensing Technology (ICST)*, Auckland, 8–10 Dec. 2015.
146. Rosli, A.B.; Shariffudin, S.S.; Awang, Z.; Herman, S.H. Deposition temperature dependence of ZnO nanostructures growth using TCVD for EGFET pH sensor, *IEEE Regional Symposium on Micro and Nanoelectronics (RSM)*, Batu Ferringhi, Malaysia, 23–25 Aug., 2017
147. Ahmed, N.M.; Kabaa, E.A.; Jaafar, M.S.; Omar, A.F. Characteristics of extended–gate field–effect transistor (EGFET) based on porous n–type (111) silicon for use in pH sensors, *Journal of Electronic Materials* **2017**, *46:10*, 5804–5813. 10.1007/s11664–017–5604–8.

148. Rasheed, H.S.; Ahmed, N.M.; Matjafri, M.Z. Ag metal mid layer based on new sensing multilayers structure extended gate field effect transistor (EG–FET) for pH sensor, *Materials Science in Semiconductor Processing* **2018**, *74*, 51–56. 10.1016/j.mssp.2017.10.011.
149. Arafa, H.; Obahiagbon, U.; Kullman, D.; Dominguez, F–J.; Magee, A.; Christen, J.B. Characterization and application of a discrete quartz extended–gate ISFET for the assessment of tumor cell viability, International Conference on Electrical, *Electronics and System Engineering (ICEESE)*, Kuala Lumpur, Malaysia, 9–10 Dec. 2014.
150. Shalmany, S.H.; Merz, M.; Fekri, A.; Chang, Z–Y.; Hoofman, R.J.O.M.; Pertijs, M.A.P. A 7μW offset–and temperature–compensated pH–to–digital converter, *Journal of Sensors* **2017**, *2017*, 1–8. 10.1155/2017/6158689
151. Lin, M–Y.; Hsu, W–Y.; Yang, Y–S.; Huang, J–W.; Chung, Y–L.; Chen, H. Immobilized rolling circle amplification on extended–gate field–effect transistors with integrated readout circuits for early detection of platelet–derived growth factor, *Analytical Bioanalytical Chemistry* **2016**, *408:17*, 4785–4797. 10.1007/s00216–016–9568–y.
152. Choi, J.; Lee, H.H.; Ahn, J.; Seo, S.; Shin, J. Differential–mode biosensor using dual extended–gate metal–oxide–semiconductor field–effect transistors. *Japanese Journal of Applied Physics* **2012**, *51*, 06FG05–1 – 06FG05–5. 10.1143/JJAP.51.06FG05.
153. Chen, P.; Yin, L.; Cho, T. Optical and impedance characteristics of EGFET based on SnO2/ITO sensing gate. *Life Science Journal* **2014**, *11*, 871–875.
154. Sanches Nascimento, R.A.; Mulato, M. Mechanisms of Ion Detection for FET–Sensors Using FTO: Role of Cleaning Process, pH Sequence and Electrical Resistivity. *Materials Research* **2017**, *20*, 1369–1379. 10.1590/1980–5373–mr–2017–0502.
155. Batista, P.D.; Mulato, M. Polycrystalline fluorine–doped tin oxide as sensoring thin film in EGFET pH sensor. *Journal of Material Science* **2010**, *45*, 5478–5481. 10.1007/s10853–010–4603–4.
156. Guidelli, E.J.; Guerra, E.M.; Mulato, M. V2O5/WO3 mixed oxide films as pH–EGFET sensor: sequential re–usage and fabrication volume analysis. *ECS Journal of Solid State Science and Technology* **2012**, 1:3, (2012), N39–N44. 10.1149/2.007203jss.
157. Kajisa, T.; Sakata, T. Monitoring of hydroxyapatite crystal formation using field–effect transistor. *Japanese Journal of Applied Physics* **2016**, *55*, 04EM09–1 – 04EM09–5.
158. Sabah, F.A.; Ahmed, N.M.; Hassan, Z.; Almessiere, M.A. A novel CuS thin film deposition method by laser–assisted spray photolysis deposition and its application to EGFET. *Sensors and Actuators B: Chemical* **2017**, *247*, 197–215. 10.1016/j.snb.2017.03.020.
159. Tsai, W.; Huang, B.; Yang, P.; Wang, K.; Hsiao, C.; Cheng, H. Oxygen plasma functionalized multiwalled carbon nanotube thin film as a pH sensing membrane of extended–gate field–effect transistor. *IEEE Electron Device Letters* **2013**, *34*, 1307–1309. 10.1109/LED.2013.2278214.